

Ising model with periodic pinning of mobile defects

M. Holschneider and W. Selke

Institut für Theoretische Physik, Technische Hochschule, D-52056 Aachen, Germany

A two-dimensional Ising model with short-range interactions and mobile defects describing the formation and thermal destruction of defect stripes is studied. In particular, the effect of a local pinning of the defects at the sites of straight equidistant lines is analysed using Monte Carlo simulations and the transfer matrix method. The pinning leads to a long-range ordered magnetic phase at low temperatures. The dependence of the phase transition temperature, at which the defect stripes are destabilized, on the pinning strength is determined. The transition seems to be of first order, with and without pinning.

PACS numbers: 05.10.Ln, 05.50+q, 74.72.Dn, 75.10.Hk

I. INTRODUCTION

Striped magnetic structures in high-temperature superconductors and related materials have attracted much interest for more than a decade, both theoretically and experimentally [1, 2, 3, 4, 5, 6]. In that context, motivated by recent experiments on $(\text{Sr}, \text{Ca}, \text{La})_{14}\text{Cu}_{24}\text{O}_{41}$ [7, 8], a class of rather simple two-dimensional Ising models has been introduced describing the formation and thermal destruction of defect stripes [9].

The model consists of spin-1/2 Ising variables, mimicking Cu^{2+} ions, and non-magnetic defects, $S = 0$, corresponding to holes. The spins are arranged in chains with antiferromagnetic interactions, $J_a < 0$, between neighboring spins in adjacent chains. Along the chains, neighboring spins are coupled ferromagnetically, $J > 0$, while next-nearest neighbor spins separated by a defect interact antiferromagnetically, $J_0 < 0$. The defects are allowed to move along the chain through the crystal. The mobility of the defects is determined by the changes in the magnetic energy encountered during their motion (annealed Ising model).

In a 'minimal variant' of the model, the couplings in the chains, J and $|J_0|$, are assumed to be indefinitely strong. The minimal model has been shown to describe the formation of defect stripes, oriented perpendicular to the chains, whose coherency gets destroyed at a phase transition. At the transition, one observes a pairing effect for the defects in the chains, reflecting an effectively attractive interaction between defects mediated by the magnetic interaction between the chains, J_a . The thermal behavior of the full model, choosing experimentally realistic values of the couplings in the chains, resembles closely that of the minimal model [9].

The aim of this paper is to study the impact of a local defect pinning energy of strength E_p on thermal properties of the minimal model. In the experimentally studied $(\text{Sr}, \text{Ca}, \text{La})_{14}\text{Cu}_{24}\text{O}_{41}$ compounds [7, 8], holes are pinned by Ca- or La-ions, which, in turn, are rather immobile. In the following, we assume that the fixed pinning sites form straight equidistant lines perpendicular to the chains, with the number of pinning sites being

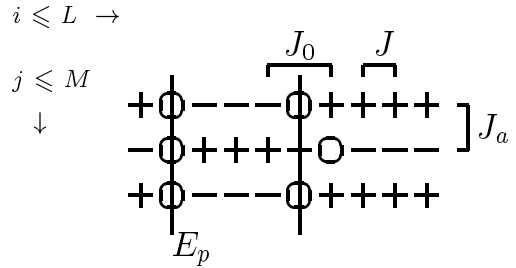


FIG. 1: Sketch of the interactions in the Ising model on a square lattice with periodic pinning of mobile defects.

equal to the number of defects. Beyond the specific experimental motivation, the model is hoped and believed to be of genuine theoretical interest.

Of course, the model still allows for thermal fluctuations of the defect stripes at finite pinning strength. Indeed, the instability of the defect stripes and the effects of the pinning on the spin ordering are intriguing features of the present model. In particular, at low temperatures spin correlations are expected to become long-ranged for non-vanishing pinning, while they decay algebraically when $E_p = 0$ [9]. The dependence of the phase transition, at which the defect stripes get destroyed, on E_p is an interesting aspect of the model as well. Without pinning, the transition temperature had been estimated, but the type of the transition had not been studied.

The layout of the paper is as follows. In the next section, we shall introduce the model and the methods, Monte Carlo simulations and transfer matrix calculations. Results will then be presented and discussed in Sect. III. Finally, a short summary concludes the article.

II. MODEL AND METHODS

We consider an Ising model on a square lattice, setting the lattice constant equal to one. Each lattice site (i, j) is occupied either by a spin, $S_{i,j} = \pm 1$, or by a



FIG. 2: Typical Monte Carlo equilibrium configurations of the minimal model, $\Theta = 0.1$ and $q_p = 1.0$, of size $L = M = 40$ at temperatures $k_B T/|J_a| = 0.8$ (a), 2.3 (b), and 2.9 (c). Only parts of the systems are shown.

defect corresponding to spin zero, $S_{i,j} = 0$, see Fig. 1. The defects are mobile along one of the axes of the lattice, the chain direction. The sites in the j -th chain are denoted by (i, j) . We assume a ferromagnetic coupling, $J > 0$, between neighboring spins, $S_{i,j}$ and $S_{i\pm 1,j}$, along the chain, augmented by an antiferromagnetic interaction, $J_0 < 0$, between those next-nearest spins in the same chain, which are separated by a defect. Spins in adjacent chains, $S_{i,j}$ and $S_{i,j\pm 1}$, are coupled antiferromagnetically, $J_a < 0$. Usually a minimal distance of two lattice spacings between neighboring defects in a chain is assumed, i.e. two defects are separated by at least one spin due to strong short range repulsion between defects (alternatively, one may introduce an additional ferromagnetic coupling between spins separated by a pair of nearest-neighboring defects). A local pinning potential acts on the defects, lowering the energy of the defects at fixed sites by an amount E_p . In the following, we choose pinning sites along equidistant straight lines, $i = i_p$, perpendicular to the chains with the number of pinning sites being equal to the number of defects, N_d . Accordingly, the Hamiltonian of the model may be written as

$$\mathcal{H} = - \sum_{ij} [J S_{i,j} S_{i\pm 1,j} + J_0 S_{i,j} S_{i\pm 2,j} (1 - S_{i\pm 1,j}^2) + J_a S_{i,j} S_{i,j\pm 1} + E_p (1 - S_{i,j}^2) \delta_{i,i_p}], \quad (1)$$

see Fig. 1. We assume that the number of defects is the same in each chain, determined by the defect concentration Θ , denoting the total number of defects divided by the total number of sites, N_d/N . In this study, we set $\Theta = 0.1$, where the distance between the pinning lines is then ten lattice spacings.

In the following we consider the 'minimal' variant of the model by assuming the couplings in the chain, J and

$|J_0|$, to be indefinitely strong [9]. Thence the spins form intact clusters in the chains between two consecutive defects, and neighboring spin clusters have opposite sign. Thermal quantities depend only on, say, $k_B T/|J_a|$ and the ratio $q_p = E_p/|J_a|$.

To study the minimal model with pinning of mobile defects, we used Monte Carlo techniques [10] and the transfer matrix method [11].

In the simulations, a new configuration of spins and defects may be generated by exchanging a defect with a neighboring spin in a chain, reversing the sign of the spin to keep intact spin clusters. The energy change associated with this elementary process is determined by J_a and E_p , see the Hamiltonian (1). As usual, the related Boltzmann factor determines the probability of accepting the new configuration [10]. Of course, simulations are performed on finite lattices with $N = L \times M$ sites, L being the number of sites in a chain. We shall present results for $L = M$. We employ full periodic boundary conditions. To investigate finite size effects, the linear dimensions, L and M , were varied from 20 to 320. Typically, runs of at least a few 10^6 Monte Carlo steps per defect were performed, averaging then over such realizations to estimate error bars. The pinning strength, $q_p = E_p/|J_a|$, ranged from 0 to 2.0.

The transfer matrix calculations were done in the standard way [11] with the matrices representing the interactions of the entire chains. All eigenvalues and eigenvectors were computed numerically, enabling us to derive quantities for arbitrary M , being finite or infinite. Studying the case $\Theta = 0.1$, L was chosen to be 20, with two defects per chain. Larger systems, i.e. with L being at least 40, are outside the current reach of computer facilities. Of course, one may study the case of more than two defect stripes in the case of $L = 20$ by enlarging the

defect concentration. We shall consider here, however, only the case of a fixed value of $\Theta = 0.1$. q_p ranged from 0 to 5.0.

Physical quantities of interest include the specific heat, C , and spin correlation functions (depending, in general, on the distance from the pinning lines, i.e. on i), parallel to the chains,

$$G_1(i, r) = \left(\sum_j \langle S_{i,j} S_{i+r,j} \rangle \right) / L, \quad (2)$$

and perpendicular to the chains,

$$G_2(i, r) = \left(\sum_j \langle S_{i,j} S_{i,j+r} \rangle \right) / L, \quad (3)$$

considering systems with $M = L$. Without pinning, the defects are expected to be delocalized so that there is full translational invariance, and the spin correlations do not depend on i . Note that in the thermodynamic limit for infinitely large distance, $r \rightarrow \infty$, the perpendicular correlations $G_2(r)$ determine the profile of the squared magnetization

$$m^2(i) = \lim_{L \rightarrow \infty} m_L^2(i) = \lim_{L \rightarrow \infty} G_2(i, L/2) \quad (4)$$

We also calculated less common microscopic quantities which describe the stability of the defect stripes and the ordering of the defects in the chains. In particular, we computed the average minimal distance, d_m , between each defect in chain j , at position (i_d, j) , and those in the next chain, at $(i'_d, j + 1)$, i.e.

$$d_m = \sum_{i_d} \langle \min |i_d - i'_d| \rangle / N_d, \quad (5)$$

dividing the sum by the number of defects, N_d . Furthermore, we calculated the cluster distribution, $n_d(l)$, denoting the probability that consecutive defects in a chain are separated by l spins, in analogy to the distribution of cluster lengths in percolation theory [12]. Our main emphasis will be on pairs of defects with $l = 1$. Finally, it turned out to be quite useful to visualize the microscopic spin and defect configurations as encountered during the simulation.

III. RESULTS

In the ground state, $T = 0$, of the minimal model, the defects form straight stripes perpendicular to the chains, separating antiferromagnetic domains of spins. Without pinning, $E_p = 0$, the ground state is highly degenerate. Each arrangement of defect stripes separated by at least

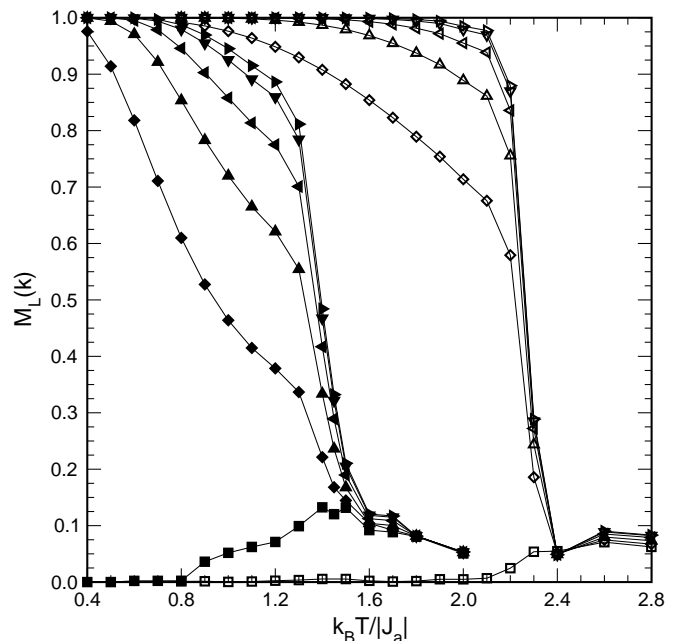


FIG. 3: Profiles of the absolute magnetization $M_L(k)$, at pinning strength $q_p = 0.2$ (full symbols) and 2.0 (open symbols), with $k = 1$ (squares), 2 (diamonds), 3 (triangles up), 4 (triangles left), 5 (triangles down) and 6 (triangles right). Results have been obtained from simulations of systems of size $L = M = 160$.

two lattice spacings has the same lowest possible energy, resulting in an exponential decay of the correlations G_1 parallel to the chains, while the spins are perfectly correlated perpendicular to the chains [9]. By introducing the pinning potential, $E_p > 0$, the defect stripes coincide with the pinning lines, at $i = i_p$. Obviously, G_1 continues to oscillate, but now with a constant amplitude. Of course, the spin correlations perpendicular to the chains, $G_2(r)$, are equal to 1 for even distances r and -1 for odd distances r , when staying away from the pinning lines, i_p .

Increasing the temperature, $T > 0$, the defects are allowed to move so that the stripes start to meander and finally break up, as exemplified in typical Monte Carlo configurations depicted in Fig. 2. Due to the pinning the defects tend to stick to the pinning lines at low temperatures. The detachment or depinning of the defects from those lines is expected to occur without phase transition, as had been shown in the framework of SOS models with pinning [13]. The mapping of the minimal model onto the standard SOS model has been discussed before [9]. However, once the defects take positions far from the pinning sites, the magnetic interactions may mediate effectively attractive couplings between the defects. As for vanishing pinning [9], these couplings, absent in standard SOS models, may eventually destroy the coherency of the defect stripes through a phase transition, as will be discussed below. We shall provide numerical evidence that the transition is of first order. The effect of the pin-

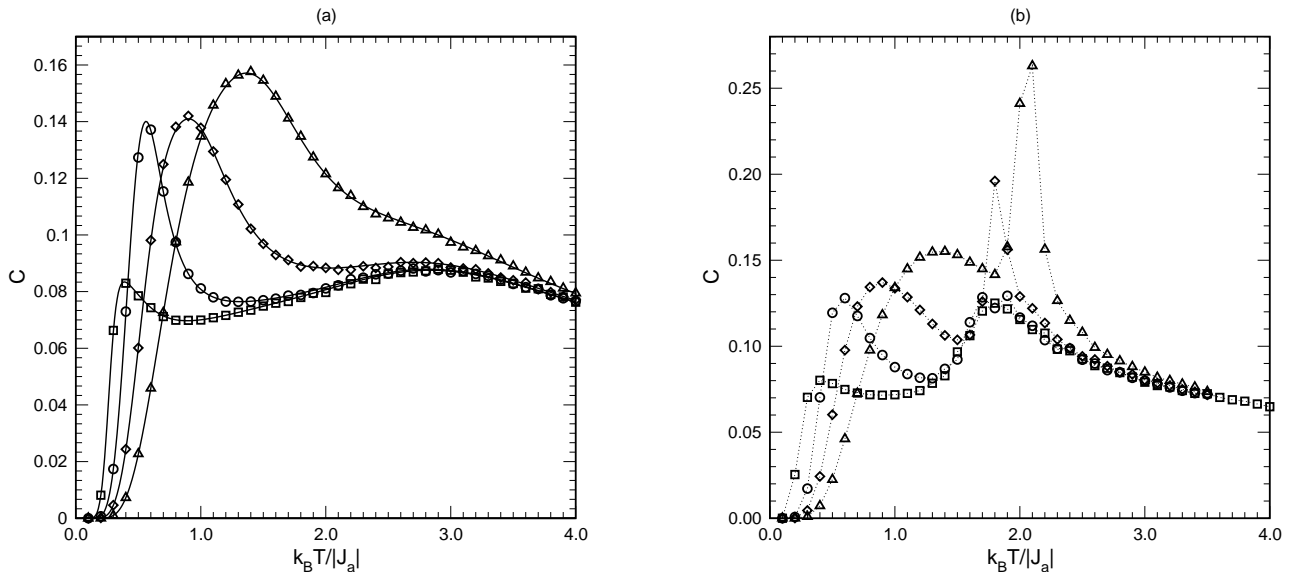


FIG. 4: Specific heat, C , at $q_p = 0$ (squares), 0.2 (circles), 0.5 (diamonds), and 1.0 (triangles), for systems of size (a) $L = M = 20$, showing results from transfer matrix calculations (solid line) and simulations, and of size (b) $L = M = 80$, obtained from simulations.

ning on the meandering and breaking up of the stripes, for various physical quantities, is exemplified in Figs. 3 to 7. Note that in most of the figures we did not include error bars since they were, typically, not larger than the size of the symbols. Such a statement would not hold for appreciably shorter Monte Carlo runs because of the rather slow fluctuations of the defect stripes.

At $T > 0$, without pinning, $E_p = 0$, the model shows no magnetic long-range order. The spin correlation function parallel to the chains, G_1 , has been shown, doing a free-fermion calculation, to decay algebraically at low temperatures [9]. Indeed, our new Monte Carlo results both for G_1 and G_2 are consistent with such an algebraic decay in the low-temperature phase characterized by meandering defect stripes whose positions can fluctuate rather freely. In particular, for finite systems of size $L \times L$, the profile of the absolute value of the magnetization, $|m_L(i)| = \sqrt{m_L^2(i)}$, reflects the translational invariance, i.e. it does not depend on i , and it decreases significantly with increasing system size L . In marked contrast, with pinning, $E_p > 0$, at low temperatures long-range magnetic order sets in, as seen easily from the profiles of the absolute magnetization between two pinning lines. The profiles are denoted in the following by $M_L(k)$ with k running from 1 to 11; $k = 1$ and $k = 11$ denote the two pinning lines, the center line in between them is at $k = 6$. Obviously, one has $M_L(12 - k) = M_L(k)$ for reasons of symmetry. Examples of pertinent profiles are displayed in Fig. 3 at weak, $q_p = 0.2$, and strong, $q_p = 2.0$, pinning. Long-range order at low temperatures follows from the fact that the magnetization especially near the center between the two pinning lines is largely independent of system size. At high temperatures, the magnetiza-

tion decreases appreciably with increasing system size, tending to zero in the thermodynamic limit. Indeed, finite-size analyses allow one to locate the phase transition temperature as a function of the pinning strength, $T_c(q_p = E_p/|J_a|)$. Estimates agree with those obtained from analyses of the specific heat C , to be discussed next. Note that $M_L(k)$ (or an average over these absolute line magnetizations) may be considered as the order parameter of the problem.

Results for the specific heat C are depicted in Figs. 4a and 4b for lattices with linear dimension $L = 20$ and 80 at pinning $0 \leq q_p \leq 1.0$. At fixed pinning and varying temperature, one observes two maxima in C . The maximum at the lower temperature is almost independent of the system size, and it stems from the meandering of the defects stripes with few excitations, i.e. a small kink density, as we checked by analysing and simulating corresponding SOS or TSK (terrace-step-kink) models [13, 14, 15] with pinning, similarly to the case without pinning [9]. The lower maximum is shifted towards higher temperatures when increasing the pinning strength E_p . It may eventually be masked by the upper maximum. The upper maximum of C , occurring at $T_{\max}(L)$, signals the instability of the defect stripes due to thermally excited large fluctuations of the defect positions. At strong pinning, these fluctuations are expected to set in once the defects start to detach in significant numbers from the pinning lines, giving then rise to a large specific heat, see Fig. 4b. In any event, the height of the second maximum increases clearly with increasing system size, indicating a phase transition in the thermodynamic limit, $L \rightarrow \infty$. To estimate the transition temperature, we plotted $T_{\max}(L)$ versus $1/L$, with

L going up to 160, see Fig. 5. From a linear extrapolation one may approximate the phase transition temperature $T_c(q_p) = T_{\max}(L = \infty)$. $T_c(q_p)$ is found to increase monotonically with q_p . More specifically, we obtain the following estimates from the data depicted in Fig.5.: $k_B T_c(q_p)/|J_a| = 1.1 \pm 0.1$ at $q_p = 0.2$ (being close to the estimate at $q_p = 0$ [9]), 1.30 ± 0.1 at $q_p = 0.5$, 1.55 ± 0.1 at $q_p = 1.0$, and 2.10 ± 0.05 at $q_p = 2.0$, with error bars reflecting some of the uncertainty in the linear extrapolation. Finite size analyses for other quantities lead to similar estimates for the possible transition temperature, as already mentioned in context of the magnetization profiles.

With pinning, the magnetization changes more and more drastically for larger systems close to $T_{\max}(L)$, compare to Fig. 3. This behavior may suggest that in the thermodynamic limit the phase transition is of first order, with a jump in the magnetization at T_c . To clarify this aspect, we determined the perpendicular correlation length, following from G_2 , when approaching T_c from high temperatures. The correlation length may be estimated from analyzing the function [16]

$$\xi_{\text{eff}}(r) = - \left(\frac{d(\ln G_2(r))}{d(r)} \right)^{-1}$$

with $G_2(r) = \sum_i |G_2(i, r)|/L$ (6)

Typically, the 'effective correlation length' $\xi_{\text{eff}}(r)$ increases rather quickly monotonically for small r until it acquires a plateau-like behavior, and finally it rises steeply due to the finite size effect and periodic boundary conditions. Obviously, at a plateau of height ξ_0 , one has $G_2 \propto \exp(-r/\xi_0)$. Indeed, in the thermodynamic limit for $T > T_c$, the height of the plateau at large r obviously corresponds to the standard correlation length ξ . Much care is needed close to the transition because very large system sizes may have to be studied to get an extended plateau. From simulations of systems with $L = M = 160$, we determined the correlation length versus temperature, at various fixed q_p . Using linear extrapolation near $T_c(q_p)$, see above, we estimate the perpendicular correlation length at the transition. It is found to increase from about 20 lattice spacings at $E_p/|J_a| = 2.0$ to about 30 lattice spacings at $E_p = 0$; i.e., it is finite. This finding supports the suggestion that the destruction of the defect stripes occurs through a phase transition of first order, with and also without pinning. A remark of caution may be added for the case of vanishing pinning. There, spin correlations in the low-temperature phase decay algebraically, and one might expect a transition of Kosterlitz-Thouless type. As has been noted before, however, algebraic order can be also destroyed by a transition of first order [17, 18].

The destruction of the defect stripes can be seen rather directly in the average minimal distance between defects in adjacent chains, d_m . In Fig. 6, simulational data for

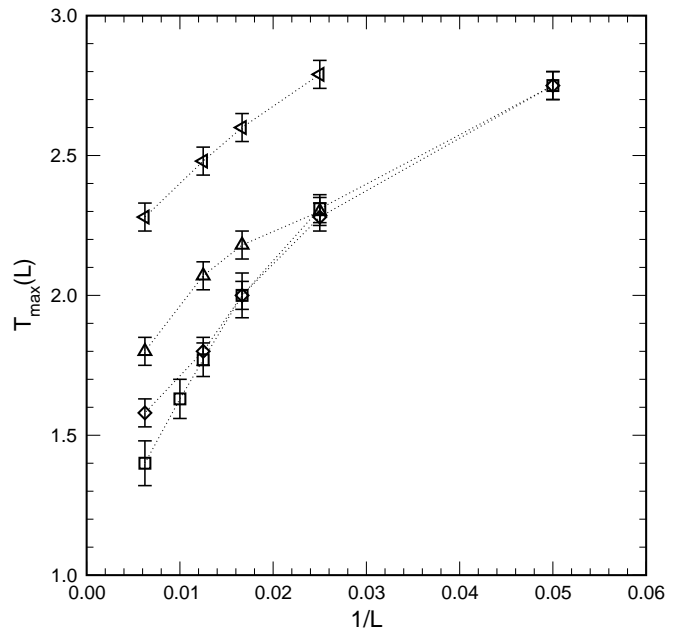


FIG. 5: Size dependence of the location of the maximum in the specific heat, $T_{\max}(L)$, as obtained from simulations, at $q_p = 0.2$ (squares), 0.5 (diamonds), 1.0 (triangles up), and 2.0 (triangles left) for $L = M$ ranging from 20 to 160.

system sizes $L = M$ ranging from 20 to 160, at $q_p = 2.0$, are displayed. The temperature dependence of d_m resembles closely the one found for the model without pinning [9]. While at low temperatures $d_m(T)$ does not depend significantly on the system size, it starts to rise rapidly at some characteristic temperature, corresponding to $T_{\max}(L)$ in the case of the specific heat, with the height of the maximum in the temperature derivative of d_m increasing strongly with larger system size. The location of the maximum, signalling the breaking up of the stripes, moves to lower temperatures as L gets larger. The quantitative behaviour is quite similar to the one of the specific heat and the magnetization profiles, for the various pinning strengths $q_p = 0, 0.2, 0.5, 1.0$, and 2.0 .

The destabilization of the stripes seems to be driven by effectively attractive couplings between consecutive defects in a chain, mediated by the spin interactions J_a (possibly reminiscent of the spin-bag mechanism [19]). Indeed, effectively attractive couplings may occur when two such defects, say, in chain j , at sites (i, j) and $(i + m, j)$, are displaced strongly with respect to corresponding defects in adjacent chains, $j \pm 1$, so that the spins in those chains at sites in between $(i, j \pm 1)$ and $(i + m, j \pm 1)$ have the same sign as the spins between the two defects in chain j . Such a situation may be realized, for instance, when three defects in chain j are in a cage of four defects in total, at, say, sites $(i, j \pm 1)$ and $(i + k, j \pm 1)$, in the neighboring chains with spin clusters of the same sign between the two pairs of defects in these chains $j - 1$ and $j + 1$. Then two of the three defects in the cage will move towards each other [9]. In

any event, due to the effectively attractive coupling, mediated by J_a , two consecutive defects in chain j tend to form a pair of next-nearest neighboring defects having the minimal separation distance of two lattice spacings. The temperature and size dependence of the probability to find such pairs of defects, given by the pair probability $n_d(l=1)$, is depicted in Fig. 7, at fixed pinning strength, $q_p = 2.0$, and various system sizes. In general, the pronounced increase of the pair probability occurs close to the temperature $T_{\max}(L)$, where other quantities signal the thermal instability of the defect stripes as well. For larger system sizes the increase in $n_d(1)$ gets sharper and sharper in accordance with a transition of first order. At strong pinning, the pair probability rises quite drastically already in systems of moderate size, see Fig. 7, possibly reflecting the moderate correlation length at the transition, as discussed above.

Note that the type of stripe instability we observe here is not included in standard descriptions of wall instabilities in two dimensions [17, 20, 21, 22], where either the number of walls is not fixed, giving rise to incommensurate structures, or dislocations play an important role in the context of melting of crystals. Also the bunching of steps in TSK models with attractive step-step interactions [23] or instabilities in polymer filaments due to attractive couplings [24, 25] are rather different from the destruction of defect stripes due to the pairing of defects induced by the inter-chain magnetic interactions J_a .

IV. SUMMARY

In this paper a two-dimensional Ising model with periodic local pinning of mobile defects has been studied. Albeit the model has been motivated by recent experiments on cuprates with low-dimensional magnetic interactions, the model is believed to be of genuine theoretical interest as well.

In particular, based on Monte Carlo simulations and transfer matrix calculations, the model is found to describe the pinning, meandering and, finally at higher temperatures, the destruction of defect stripes.

The pinning gives rise to a long-range ordered magnetic phase at low temperatures while magnetic correlations decay algebraically at low temperatures without pinning.

The thermal instability of the defect stripes, which had been already identified for vanishing pinning, shifts towards higher temperatures as the pinning strength

increases. The instability is signalled by pronounced anomalies, among others, in the specific heat, in the magnetization profile, in the probability of defect pairs with shortest separation distance, and in the average minimal distance between defects in neighboring chains. The breaking up of the stripes is caused by an effectively attractive coupling between the defects mediated by the inter-chain interactions between spins in adjacent chains.

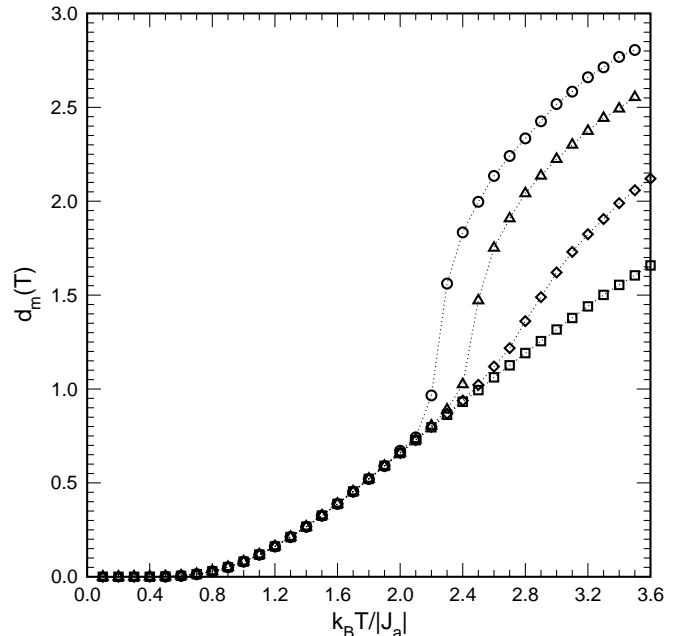


FIG. 6: Average minimal distance between defects in adjacent rows $d_m(T)$, at $q_p = 2.0$, simulating systems of size $L = M = 20$ (squares), 40 (diamonds), 80 (triangles), and 160 (circles).

We provide evidence that the stripe instability results in a phase transition of first order, accompanied, in the thermodynamic limit, by jumps in various quantities, including the magnetization profile and the correlation length. This character of the transition seems to persist for vanishing pinning.

Acknowledgments

It is a pleasure to thank B. Büchner, R. Klingeler, R. Leidl, V. L. Pokrovsky, and S. Scheidl for very helpful suggestions and discussions.

-
- [1] J. Zaanen and O. Gunnarsson, Phys. Rev. B **40**, 7391 (1989).
 - [2] H.J. Schulz, J. Phys. (Paris) **50**, 2833 (1989).
 - [3] F. Krüger and S. Scheidl, Phys. Rev. B **67**, 134512 (2003); Phys. Rev. Lett. **89**, 095701 (2002).
 - [4] C.H. Chen, S.-W. Cheong, and A.S. Cooper, Phys. Rev.

- Let. **71**, 2461 (1993); J.M. Tranquada, D.J. Buttrey, V. Sachan, and J. E. Lorenzo, Phys. Rev. Lett. **73**, 1003 (1994).
- [5] J.E. Hoffman, E.W. Hudson, K.M. Lang, V. Madhavan, E. Eisaki, S. Uchida, and J.C. Davis, Science **295**, 466 (2002).

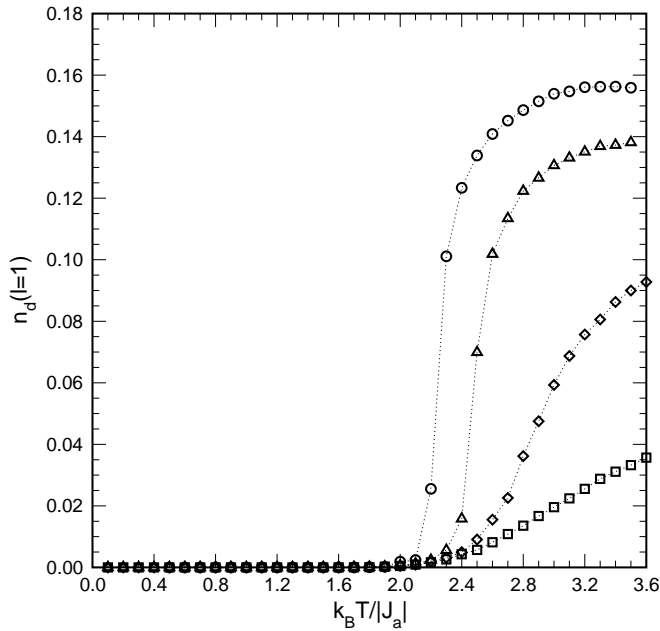


FIG. 7: Temperature dependence of the probability for pairs of neighboring defects, $n_d(l=1)$, at $q_p = 2.0$, simulating systems of size $L = M = 20$ (squares), 40 (diamonds), 80 (triangles), and 160 (circles).

[6] J. Zaanen and A.M. Oles, *Ann. Phys. (Leipzig)* **5**, 224 (1996).
 [7] U. Ammerahl, B. Büchner, C. Kerpen, R. Gross, and A. Revcolevschi, *Phys. Rev. B* **62**, R3592 (2000); A. Goukasov, U. Ammerahl, B. Büchner, R. Klingeler, T. Kroll, and A. Revcolevschi, to be published.
 [8] R. Klingeler, PhD thesis, RWTH Aachen (2003).
 [9] W. Selke, V.L. Pokrovsky, B. Büchner, and T. Kroll, *Eur.*

Phys. J. B **30**, 83 (2002).
 [10] D.P. Landau and K. Binder, *A Guide to Monte Carlo Simulations in Statistical Physics* (Cambridge, University Press, 2000).
 [11] M.P. Nightingale, in *Finite Size Scaling and Numerical Simulations in Statistical Physics*, edited by V. Privman (World Scientific, Singapore, 1990), p.287; J.M. Yeomans, *Statistical Mechanics of Phase Transitions* (Clarendon Press, Oxford, 1992).
 [12] D. Stauffer and A. Aharony, *Introduction to Percolation Theory* (Taylor and Francis, London, 1994).
 [13] G. Forgacs, R. Lipowsky, and Th.M. Nieuwenhuizen, in *Phase Transitions and Critical Phenomena*, edited by C. Domb and J. L. Lebowitz (Academic, London, 1991), Vol. 14.
 [14] W. Selke and A.M. Szpilka, *Z. Physik B* **62**, 381 (1986).
 [15] T.L. Einstein, H.L. Richards, S.D. Cohen, and O. Pierre-Louis, *Surf. Sci.* **493**, 460 (2001).
 [16] W. Selke, *Physica A* **177**, 460 (1991); W. Selke, N.M. Svrakic, and P.J. Upton, *Z. Physik B* **89**, 231 (1992).
 [17] D.R. Nelson and B.I. Halperin, *Phys. Rev. B* **19**, 2457 (1979).
 [18] P. Minnhagen, *Rev. Mod. Phys.* **59**, 1001 (1987).
 [19] J.R. Schrieffer, X.G. Wen, and S.C. Zhang, *Phys. Rev. Lett.* **60**, 944 (1988); A. Kampf and J.R. Schrieffer, *Phys. Rev. B* **41**, 6399 (1990).
 [20] V.L. Pokrovsky and A.L. Talapov, *Phys. Rev. Lett.* **42**, 65 (1979).
 [21] J. Villain, D.R. Grempel, and J. Lapujoulade, *J. Phys. F* **15**, 809 (1985).
 [22] B.N.J. Persson, *Surf. Sci. Rep.* **15**, 1 (1992).
 [23] D.J. Liu and J.D. Weeks, *Phys. Rev. Lett.* **79**, 1694 (1997).
 [24] T.W. Burkhardt and P. Schlottmann, *J. Phys. A* **26**, L501 (1993).
 [25] R. Bundschuh, M. Lässig, and R. Lipowsky, *Eur. Phys. J. E* **3**, 295 (2000).